Calibration of Resolver Sensors in Electromechanical Braking Systems: A Modified Recursive Weighted Least-Squares Approach

Reza Hoseinnezhad, Alireza Bab-Hadiashar, *Senior Member, IEEE*, and Peter Harding

***Abstract*—Resolver sensors are utilized as absolute position transducers to control the position and speed of actuators in many industrial applications. The accuracy and convergence of the position and speed measurements provided by resolvers in electromechanical braking system (EMB) designs directly contribute to the braking performance and vehicle safety. In practice, the dc drifts, amplitudes, and phase shift of the resolver signals vary with aging and temperature, and adaptive techniques are required for the calibration of these parameters of resolvers. Existing classical adaptive techniques such as recursive least squares are unable to track the parameters during resting (low-speed actuation or stationary) periods and also a transient period after them. This paper proposes a new approach for real-time tracking of resolver parameters specially developed for actuator-control applications with varying speed and long resting periods. We formulate the algebraic relationship between the resolver parameters and the parameters of resolver characteristic ellipse, which is the ellipse formed by plotting the resolver signals versus each other. Having known the characteristic ellipse parameters, the resolver parameters are calculated using the formulated algebraic relation. Then, a new recursive and adaptive estimator is proposed to track the parameters of characteristic ellipse. The low computational complexity of the proposed method makes it desirable for real-time applications like the EMBs, where limited computational power and memory are available. Experimental results show that the proposed technique is able to track the resolver parameters and the accurate actuator position with a small error in real-time, while other adaptive estimators are unable to track the resolver parameters during and after resting periods.**

***Index Terms*—Adaptive estimation, braking, calibration, parameter estimation, recursive estimation.**

I. Introduction

DIGITAL signal processors have enabled sensorless control that reduces the total system operating cost by eliminating mechanical sensors while maintaining the performance of the control system. However, there are still applications where sensorless control cannot achieve the required accuracy and reliability. This is especially true with respect to the angular position and speed. Examples include servo applications like robotics and numerically controlled machine tools. Mechanical sensors used in such applications are usually incremental encoders and resolvers. While incremental encoders are relative position sensors, absolute encoders are expensive and complicated. On the other hand, resolvers are low cost and simple absolute angle transducers, providing two output signals that always allow the detection of the absolute angular position [1]–[3]. In addition, resolvers suppress common-mode noise and are especially useful in noisy environments.

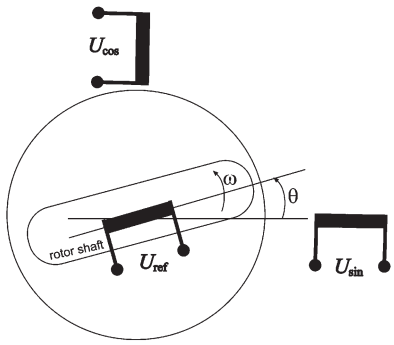

Fig. 1. Schematic diagram of the basic operation of a resolver.

Resolvers are rotary transformers with one rotating reference winding (supplied by $U_{\rm ref}$) and two stator windings (Fig. 1). The reference winding is fixed on the rotor and rotates jointly with the shaft. Two stator windings are placed in quadrature of one another to generate the sine and cosine voltages ($U_{\rm sin}$ and $U_{\rm cos}$), respectively. The sine winding is phase advanced by 90° with respect to cosine winding. The frequency of $U_{\rm sin}$ and $U_{\rm cos}$ is identical to the reference voltage, and their amplitudes vary according to the sine and cosine of the shaft angle θ. Both windings will be further referred to as output windings.

A. Resolvers in Electromechanical Braking Systems (EMBs)

The resolvers have become an increasingly important part of brake-by-wire systems. Brake-by-wire is a frontier technology that will allow many braking functions to switch to electronic actuation and control. When implemented by an EMB system, a brake-by-wire system includes four electric calipers (e-calipers). A schematic diagram of the main components of an e-caliper is shown in Fig. 2.

Once the driver inputs a brake command to the system via a human–machine interface—HMI (e.g., the brake pedal), four

Manuscript received March 13, 2006; revised May 23, 2006. Abstract published on the Internet January 27, 2007. This work was supported in part by the Research Centre for Advanced By-Wire Technologies (RABiT) and in part by Pacifica Group Technologies Pty Ltd., Australia.

R. Hoseinnezhad and A. Bab-Hadiashar are with the Faculty of Engineering and Industrial Sciences, Swinburne University of Technology, Hawthorn, VIC 3122, Australia (e-mail: rhoseinnezhad@swin.edu.au).

P. Harding is with Pacifica Group Technologies Pty Ltd., East Bentleigh, VIC 3165, Australia.

Digital Object Identifier 10.1109/TIE.2007.893049

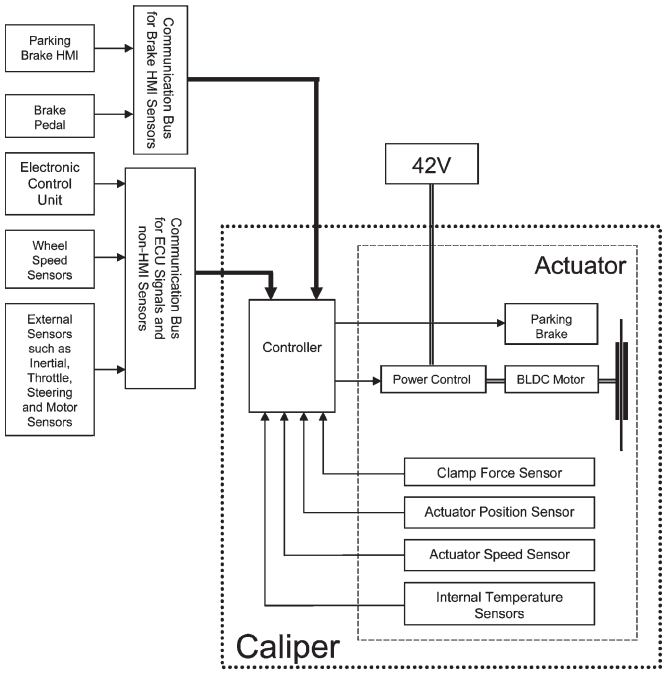

Fig. 2. Schematic diagram of the main components of an e-caliper and their connections to other components in an EMB system.

independent brake commands are generated by the electronic control unit (ECU) based on high-level brake functions such as antilock braking system (ABS) or vehicle stability control (VSC) [4], [5]. These command signals are sent to the four e-calipers via a communication network. As this network might not be able to properly communicate with the e-calipers due to network faults, HMI sensory data are also directly transmitted to each e-caliper via a separate data bus.

In each e-caliper, a controller uses the brake command (received from ECU) as a reference input. The controller provides drive-control commands for a power control module. This module controls three-phase drive currents for a brake actuator that is a permanent-magnet dc motor, usually energized by 42-V sources. In addition to tracking its reference brake command, the caliper controller also controls the position and speed of the brake actuator. Thus, two sensors are required to measure the position and speed of the actuator in each e-caliper. Because of the safety-critical nature of the application, even missing a limited number of samples of sensory data should be compensated for. Hoseinnezhad and Bab-Hadiashar have proposed a new memory-efficient method with a low computational overhead to compensate for the missing samples of such sensory data [6]. Among different sensors in the e-caliper, the resolvers are of particular importance because they function as both position and speed sensors, and such measurements are critical to actuator control in each e-caliper. The following two main issues exist with using this sensor.

The first issue is with the design of a resolver-to-digital converter to extract the position and speed from the resolver outputs. Since the signals $U_{\sin}$ and $U_{\cos}$ are nonlinear functions of the position θ, nonlinear observers are required and stability of a nonlinear closed-loop observer is not always guaranteed, particularly in high-speed applications such as the EMB. Hoseinnezhad [7] has introduced a hybrid nonlinear observer with guaranteed stability for a wide range of speeds. Based on the circle theorem in the input–output nonlinear control theory, this range is analytically determined from resolver parameters.

The second issue is how to calibrate a resolver. Since the dc drifts, amplitudes, and phase shift of sine and cosine resolver signals have long-term variations with aging and short-term variations with temperature, adaptive estimators are required for updating these parameters of resolvers in real-time (calibration) [8]–[10]. To be implemented in applications like EMB systems, where limited computational power and memory space are available, simple algorithms with low computational complexity are preferred for resolver-calibration purpose. The parameter estimates given by existing classical adaptive techniques such as recursive least squares (RLS) diverge from the true parameter values during low-speed actuation and stationary periods. Such periods frequently happen in brake-by-wire actuation. Stopping the parameter estimation process during these periods is not feasible, because most of the temperature rise occurs when the brake pad is in continuous contact with the brake disk (and the actuator is at standstill), and during such periods, tracking of the resolver parameter variations with temperature is required for the purpose of actuator-position control and its stability.

This paper proposes a new approach for real-time tracking of resolver parameters specially developed for actuator-control applications with varying speed and long periods of low-speed actuation or long stationary periods, such as e-caliper control in brake-by-wire systems.

In Section II, the research problem is stated, and some related works are reviewed. Our proposed approach is explained in Section III, where we formulate the algebraic relationship between the resolver parameters and the parameters of resolver characteristic ellipse, which is the ellipse formed by plotting the resolver signals versus each other. Having known the characteristic ellipse parameters, the resolver parameters are calculated using the formulated algebraic relation. Then, a new recursive and adaptive estimator is proposed to track the parameters of characteristic ellipse. Our experimental results are presented in Section IV. Section V concludes this paper.

II. Problem Statement and Related Work

In practice, because of manufacturing variations, the stator windings axes are not perpendicular to each other. In addition, the two output signals include some dc offsets, which are not necessarily equal. Thus, the resolver output signals can be expressed as follows:

$$\begin{aligned} U_{\sin} &= A_1 \sin(\theta) + B_1 + n_1 \\ U_{\cos} &= A_2 \cos(\theta + \phi) + B_2 + n_2 \end{aligned} \tag{1}$$

where A_1 and A_2 are the sine and cosine amplitudes, B_1 and B_2 are offsets, ϕ is the phase shift due to the imperfect placement of the stator wirings, and n_1 and n_2 are measurement zero-mean

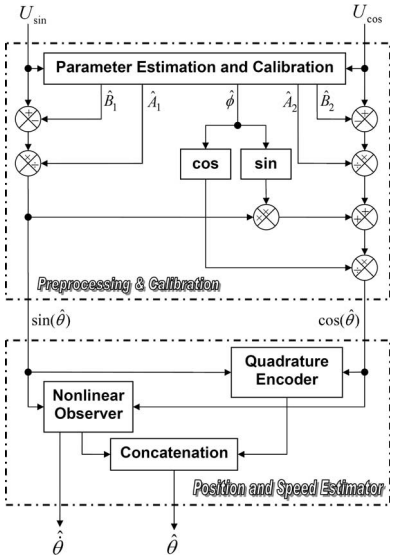

Fig. 3. Complete diagram of position and speed estimation using resolver signals, with automatic calibration of resolvers.

noise. The parameters A_1, A_2, B_1, B_2, and ϕ in (1) are called resolver parameters.

Resolver parameters gradually vary with wear and aging. Besides, in an EMB system, substantial amount of heat is generated in a brake pad, causing its temperature to rise significantly. Some of the heat is transferred to the e-caliper, and therefore, the temperature of the resolver frequently varies with braking. Indeed, this temperature variation occurs with each brake action, and in a panic brake situation, the temperature variation would even be larger than a normal brake scenario [11]. Since the resolver parameters vary with such frequent temperature variations, they should be constantly updated in real time.

If $\{\hat{A}_1, \hat{A}_2, \hat{B}_1, \hat{B}_2, \text{ and } \hat{\phi}\}$ are the estimates of the resolver parameters, then from (1), unbiased estimates of the sine and cosine of the angle are given as follows:

$$\sin(\hat{\theta}) = \frac{U_{\sin} - \hat{B}_1}{\hat{A}_1}$$
$$\cos(\hat{\theta}) = \frac{\frac{U_{\cos} - \hat{B}_2}{\hat{A}_2} + \sin(\hat{\phi})\sin(\hat{\theta})}{\cos(\hat{\phi})} \tag{2}$$

where the measurement-noise terms n_1 and n_2 have been replaced with their means (zero). Fig. 3 shows a complete diagram of the position and speed estimation, using resolver signals, that comprises two separate blocks: preprocessing and calibration and position and speed estimator, which is the core of the estimator, and its main inputs are the sine and cosine estimates given by the preprocessing and calibration block based on (2).

In the position and speed estimator block, a quadrature encoder tracks the number of quarter cycles the rotor turns by counting the zero-crossing points of the sine and cosine signals. On the other hand, the rotor speed and its position within the current quadrature (counted by the encoder) are estimated by a closed-loop nonlinear observer. A sophisticated design for such an observer has been recently reported by Hoseinnezhad [7]. The observer position estimate is added to the output of the quadrature encoder to form the total angle estimate $\hat{\theta}$.

This paper focuses on the formulation and design of the parameter estimation and calibration block in Fig. 3. Most of the techniques introduced in the literature of resolver-to-digital conversion (e.g., the works of Benammar *et al.* [12]) are useful for the realization of the position-and-speed-estimator block in Fig. 3. Hanselman [13] investigated the effects of nonideal resolver signal characteristics commonly encountered in practice and introduced expressions for the position error due to amplitude imbalance, quadrature error, inductive harmonics, reference phase shift, excitation signal distortion, and disturbance signals, and he determined the achievable bounds on the position accuracy. Bünte and Beineke [14] propose a method to suppress the systematic errors of resolvers, using Fourier analysis. In their technique, the two resolver signals form a complex signal $s(\theta(t)) = U_{\cos}(t) + jU_{\sin}(t)$, and the systematic errors are removed by compensating for the non-principal harmonics of this signal. Although their technique is simple and efficient, it is useful for applications where the offset, amplitude, and phase errors are small (the total harmonic distortion should be less than 1%). Based on this assumption, if $s(\theta(t)) = \sum_{k=-\infty}^{\infty} c_k e^{jk\theta(t)}$ is the Fourier series of the complex signal, then the coefficient c_0 represents the offset error, $\mathrm{Re}\{c_{-1}\}$ represents the amplitude difference, and $\mathrm{Im}\{c_{-1}\}$ represents the phase error. Therefore, the technique tries to minimize c_0 and c_{-1}. For the resolvers used in the EMB e-caliper, the amplitude and, particularly, the phase shifts are not small. For example, a phase shift of around 5° is observed in some of the commercial resolvers used in this application. Thus, the technique proposed by Bünte and Beineke [14] is not appropriate for calibration purposes in the e-caliper. Höscheler and Szael [15] propose a technique specifically developed for position acquisition with sinusoidal incremental encoders. In their technique, an error-detection method is also included, focusing on the removal of only the small amplitude (and not phase) errors, while the method proposed in this paper compensates for both amplitude and phase errors, whether they are large or small.

Equation (1) shows that when the resolver output signals are plotted versus each other, an elliptic contour is generated which is called, here, the characteristic ellipse of the resolver. Thus, the resolver parameter estimation can be formulated in terms of an ellipse-fitting problem. As aforementioned, real-time calibration of the resolver parameters is required, and using an adaptive estimator is unavoidable. In addition to being adaptive in real-time, we need an estimator that is able to handle the long resting periods (low-speed actuation or stationary periods) that occur during caliper movements in an EMB system. It appears that the classical and modern adaptive estimators reported in the literature (used for actuator-position tracking and control) are not intended to solve this problem and update their estimates with time and not with the distance traveled by the actuator [16]–[18]. More precisely, since the resolver parameters vary with aging and temperature and these two factors are effective when the actuator moves, the resolver-parameter estimates are required to be updated only during the motion periods and

not the resting periods, as updating the estimates during the resting periods will diverge them from their true values. We will elaborate further on this point in Section III.

It appears that most of the existing ellipse-fitting techniques have been developed for offline fitting of data samples to ellipses in applications such as pattern recognition and computer vision applications [19]–[22]. The computational complexity of such methods are too high to be applied in real-time applications like EMB systems, where limited memory and computational power are available. The most popular method used for ellipse fitting is the least squares technique.

Fitzgibbon *et al.* [19] have proposed an efficient method for fitting ellipses to the scattered data. They represent a general conic by the following implicit second-order polynomial:

$$F(\underline{a};\underline{x}) = \underline{a}^{\mathrm{T}}\underline{x} = ax^2 + bxy + cy^2 + dx + ey + f = 0 \quad (3)$$

where $\underline{a} = [a\ \ b\ \ c\ \ d\ \ e\ \ f]^{\mathrm{T}}$, $\underline{x} = [x^2\ \ xy\ \ y^2\ \ x\ \ y\ \ 1]^{\mathrm{T}}$, and $F(\underline{a};\underline{x})$ is the algebraic distance of a point (x, y) to the conic $F(\underline{a};\underline{x}) = 0$. They formulate the ellipse-fitting problem as the minimization of the following error function, which is the sum of the squared algebraic distances, subject to the elliptic constraint $4ac - b^2 > 0$:

$$E = \sum_{i=1}^{n} F(\underline{a}, \underline{x}_i) = \|D\underline{a}\|^2 \quad (4)$$

where $D = [\underline{x}_1, \underline{x}_2, \ldots, \underline{x}_n]$.

Since the parameters can be arbitrarily scaled, they incorporate the scaling into the constraint and impose the equality constraint $4ac - b^2 = 1$ and express it in the matrix form $\underline{a}^{\mathrm{T}}C\underline{a} = 1$, where C is a constant 6×6 matrix [19]. By introducing a Lagrange multiplier λ and differentiating, they arrive at the following system of simultaneous equations:

$$D^{\mathrm{T}}D\underline{a} = \lambda C\underline{a} \quad (5)$$

$$\underline{a}^{\mathrm{T}}C\underline{a} = 1 \quad (6)$$

which are the equations of a generalized eigensystem combined with the elliptic constraint. This solution is not adaptive and too complicated to be implemented in an EMB system. In addition, Fitzgibbon *et al.* assume that there are sufficient number of data samples scattered around the ellipse, and the spatial distribution of data is not included in this approach.

Chuckpaiwong [23] has applied the ellipse-fitting technique proposed by Fitzgibbon *et al.* [19] for on-site calibration of short-range radars whose signals are trigonometric functions of the distances in a form similar to (1). He specifically formulates this technique to calibrate the radar parameters on-site whenever the sensor is relocated a set of using off-line measurements, which are scattered around the ellipse. This technique cannot be applied in real-time for the adaptive calibration of resolver parameters, where frequent resting periods exist in the data samples.

In the next section, we introduce an adaptive estimator for automatic calibration of resolvers. We have modified the classical RLS technique in such a way that the parameters are updated with actuator movements instead of constant updating with time. RLS technique was chosen as the core of our new adaptive estimator for its low-computational complexity and proven convergence properties [24], [25].

III. Automatic Calibration: Proposed Approach

Merging the two equations in (1) and eliminating θ (with the noise terms removed) results in the following equation:

$$\left(\frac{U_{\cos} - B_2}{A_2\cos(\phi)}\right)^2 + \left(\frac{U_{\sin} - B_1}{A_1\cos(\phi)}\right)^2 + \frac{2\sin(\phi)}{A_1A_2\cos(\phi)^2}(U_{\sin} - B_1)(U_{\cos} - B_2) = 1. \quad (7)$$

The above equation can be formulated in the form of the following linear regression model:

$$U_{\cos}^2 = \alpha_1 U_{\sin}^2 + \alpha_2 U_{\sin}U_{\cos} + \alpha_3 U_{\sin} + \alpha_4 U_{\cos} + \alpha_5 \quad (8)$$

where $\alpha_1, \ldots, \alpha_5$ are regression parameters with the following ellipticity constraints:

$$\alpha_1 < 0 \quad \alpha_2 < 0 \quad 4\alpha_1 + \alpha_2^2 < 0. \quad (9)$$

By comparing the regression parameters in (8) with their corresponding coefficients in (7) and after some algebraic manipulation, we have derived the following equations to estimate the resolver parameters using the regression parameters:

$$\hat{\phi} = \arcsin\left(\frac{-\alpha_2}{2\sqrt{-\alpha_1}}\right) \quad (10)$$

$$\hat{B}_1 = -\frac{\alpha_3}{2\alpha_1 + \alpha_2} \quad (11)$$

$$\hat{B}_2 = \frac{\alpha_4}{2 - \alpha_2} \quad (12)$$

$$\hat{A}_2 = \frac{\sqrt{\alpha_5 + \hat{B}_2^2 - \alpha_1\hat{B}_1^2 + 2\hat{B}_1\hat{B}_2\sin(\hat{\phi})\sqrt{-\alpha_1}}}{\left|\cos(\hat{\phi})\right|} \quad (13)$$

$$\hat{A}_1 = \frac{\hat{A}_2}{\sqrt{-\alpha_1}}. \quad (14)$$

When an RLS estimator is used for resolver calibration, it minimizes the following error function in each iteration n:

$$E(n) = \sum_{i=1}^{n}\left\{\lambda^{n-i}\left(y(i) - \underline{\alpha}(n)^{\mathrm{T}} \cdot \underline{x}(i)\right)^2\right\} \quad (15)$$

where the superscript T denotes "transpose," λ is a forgetting factor to make the parameter estimates adaptive to variations with temperature and aging, $\underline{\alpha}(n) = [\alpha_1(n), \ldots, \alpha_5(n)]^{\mathrm{T}}$ is the regression parameter vector at the current iteration n, $\underline{x}(i) = [U_{\sin}(i)^2 U_{\sin}(i)U_{\cos}(i)U_{\sin}(i)U_{\cos}(i)1]^{\mathrm{T}}$ is the regression input vector, and $y(i) = U_{\cos}(i)^2$ is the regression output. To use RLS technique for resolver-parameter estimation, we need to take an additional step in each iteration n. If the ellipticity constraints (9) are satisfied, then the parameter vector $\underline{\alpha}(n)$ is updated, otherwise $\underline{\alpha}(n) = \underline{\alpha}(n-1)$.

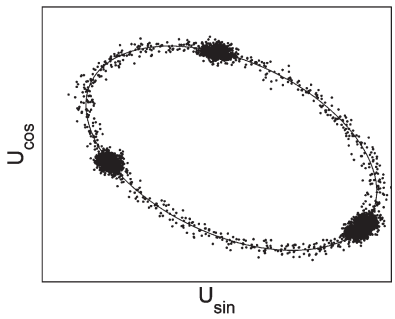

Fig. 4. Example of the distribution of resolver outputs around its characteristic curve. The lumped data points correspond with the resting periods during which the actuator stops or moves slowly.

In many real-time actuator control applications such as the EMB caliper, the data points are not evenly distributed around the characteristic ellipse of the resolver, as shown in the case example in Fig. 4, where the two output signals of a resolver used in an EMB caliper have been plotted versus each other. Particularly in an EMB system, the reference commands sent by the ECU (which are generated by high-level braking modules such as ABS, VSC, and the like [4], [5]) to the e-caliper controllers involve frequent switching between the brake (engage) and release (disengage) states. Thus, the data points sometimes move around the characteristic ellipse quickly, and during resting periods, they move slowly or even stop progressing through the contour.

During each resting period, a high density of measurements on the perimeter of the characteristic ellipse causes the RLS technique to mainly focus on fitting the ellipse to those concentrated data points. More precisely, regardless of their spatial density, all data points are equally and evenly incorporated in the estimation process by the least squares technique. In real-time actuator-control applications like EMB caliper control, a limited number of recent data samples are used by the adaptive estimator, and the spatial density of these recent samples significantly affects the performance of the estimator. We need to modify the RLS technique in such a way that the influence of each single data point is proportional to the spatial density of data points in that location so that the data are fitted to the characteristic ellipse, regardless of their spatial density around the ellipse. Without such a modification, an RLS estimator will result in wrong ellipses fitted with the concentrated data samples measured during resting periods.

Suppose that $\mathcal{N}(t)$ is the number of data samples at time t. To make the influence of each data point proportional to the inverse of the spatial density of the data at its location, we have modified the RLS-error function (15) as follows:

$$E(n)=\sum_{i=1}^{n}\left\{\lambda^{n-i}\left|\frac{d\mathcal{N}}{d\theta}\right|^{-1}\left(y(i)-\underline{\alpha}(n)^{\mathrm{T}}\cdot\underline{x}(i)\right)^{2}\right\}. \quad (16)$$

Using the chain rule, we have

$$\left(\frac{d\mathcal{N}}{d\theta}\right)^{-1}=\left(\frac{d\mathcal{N}}{dt}\right)^{-1}\frac{d\theta}{dt}. \quad (17)$$

The time derivative of N is the sampling rate and it remains constant. Thus, instead of the above error function, the following function can be minimized by the modified estimator:

$$E(n)=\sum_{i=1}^{n}\lambda^{n-i}\left\{|\hat{\omega}(i)|\left(y(i)-\underline{\alpha}(n)^{\mathrm{T}}\cdot\underline{x}(i)\right)^{2}\right\} \quad (18)$$

where $\hat{\omega}(i)$ is the speed estimate given by the nonlinear observer shown in Fig. 3. Our new estimator is a recursive weighted least-squares (RWLS) estimator with the time-varying weights $|\hat{\omega}(i)|$.

Another issue that particularly exists with resolver calibration in the real-time applications that involve frequent actuator resting periods is the forgetting process that happens during and after each resting period. On the one hand, the forgetting factor $\lambda\in(0,1)$ is needed for the estimator to be adaptive to parameter variations with aging and, more importantly, with temperature variations. As the temperature rises in each brake action and decreases afterward, the forgetting process should be fast enough for sufficient adaptivity to parameter variations. On the other hand, during resting periods, the previous data points (nicely scattered ones) are forgotten while the new data are concentrated around the resting point and not sufficiently scattered. Thus, during the resting periods and for a transient period after them, until recent data points are sufficiently scattered around the characteristic ellipse of the resolver, the RLS and RWLS estimator will result in wrong fits to the characteristic ellipse of the resolver.

To implement the forgetting process and achieve adaptivity, RLS and RWLS use an exponential scale factor of λ^{n-i}. In order to solve the problem of wrong estimates during resting periods, we have made further modification to RWLS in such a way that parameter estimates are not constantly updated with time. Indeed, they should be updated when the actuator moves so that the update process stops during resting periods. Thus, we have replaced the exponent $n-i$, which is the time passed during the interval $[i,n]$, with the total angular absolute distance traversed by the rotor during this time interval, given as follows:

$$g(i,n)=\begin{cases}\sum_{j=i+1}^{n}\left|\hat{\theta}(j)-\hat{\theta}(j-1)\right|, & i<n\\ 0, & i\geq n\end{cases} \quad (19)$$

where $\hat{\theta}$ is the position estimate given by the "position and speed estimator" block shown in Fig. 3. We call this estimator a modified RWLS (MRWLS) estimator. For MRWLS, the following error function should be minimized:

$$E(n)=\sum_{i=1}^{n}\left\{\lambda^{g(i,n)}\,|\hat{\omega}(i)|\left(y(i)-\underline{\alpha}(n)^{\mathrm{T}}\cdot\underline{x}(i)\right)^{2}\right\}. \quad (20)$$

We have formulated an iterative approach to minimize the above error function. First, we write the MRWLS error function in the form of a least-squares error function

$$E(n)=\sum_{i=1}^{n}\left(y'(i)-\underline{\alpha}(n)^{\mathrm{T}}\cdot\underline{x}'(i)\right)^{2} \quad (21)$$

where $\underline{x}'(i)$ and $y'(i)$ are auxiliary variables given as follows:

$$\underline{x}'(i) = \lambda^{\frac{g(i,n)}{2}} |\hat{\omega}(i)|^{\frac{1}{2}} \underline{x}(i)$$
$$y'(i) = \lambda^{\frac{g(i,n)}{2}} |\hat{\omega}(i)|^{\frac{1}{2}} y(i). \quad (22)$$

The parameter vector $\underline{\alpha}(n)$ that minimizes the error function (21) is the least squares solution given by the following equation:

$$\underline{\alpha}(n) = [\Phi(n)]^{-1} \underline{\Psi}(n) \quad (23)$$

where

$$\Phi(n) = \sum_{i=1}^{n} \left\{ \lambda^{g(i,n)} |\hat{\omega}(i)| \underline{x}(i) \underline{x}(i)^{\mathrm{T}} \right\} \quad (24)$$

and

$$\underline{\Psi}(n) = \sum_{i=1}^{n} \left\{ \lambda^{g(i,n)} |\hat{\omega}(i)| \underline{x}(i) y(i) \right\}. \quad (25)$$

Direct calculation of the parameters given by (23) involves a computational complexity of $O(n^2)$ that increases with time. To limit the computational requirements (similar to RLS in [24]), we derive recursive forms of (23)–(25) to iteratively estimate the parameters $\underline{\alpha}(n)$, which minimize the error function (20).

Using (19) and (24), we have

$$g(i,n) = g(i,n-1) + |\theta(n) - \theta(n-1)| \quad (26)$$

and

$$\Phi(n) = \sum_{i=1}^{n-1} \lambda^{g(i,n)} |\hat{\omega}(i)| \underline{x}(i) \underline{x}(i)^{\mathrm{T}} + |\hat{\omega}(n)| \underline{x}(n) \underline{x}(n)^{\mathrm{T}}. \quad (27)$$

Thus, $\Phi(n)$ can be recursively calculated using the following equation:

$$\Phi(n) = \lambda^{|\theta(n)-\theta(n-1)|} \Phi(n-1) + \underline{x}(n) \underline{x}(n)^{\mathrm{T}} |\hat{\omega}(n)|. \quad (28)$$

Similarly, an iterative formula for the calculation of $\underline{\Psi}(n)$, given by (25), can be obtained as follows:

$$\underline{\Psi}(n) = \lambda^{|\theta(n)-\theta(n-1)|} \underline{\Psi}(n-1) + \underline{x}(n) y(n) |\hat{\omega}(n)|. \quad (29)$$

Using the matrix inversion lemma [24] and by some algebraic manipulations, the following recursive formula is obtained:

$$\Phi^{-1}(n) = P(n) = \frac{P(n-1) - \underline{K}(n) \underline{x}(n)^{\mathrm{T}} P(n-1) |\hat{\omega}(n)|^{\frac{1}{2}}}{\lambda^{|\theta(n)-\theta(n-1)|}} \quad (30)$$

where

$$\underline{K}(n) = \frac{|\hat{\omega}(n)|^{\frac{1}{2}} P(n-1) \underline{x}(n)}{\lambda^{|\theta(n)-\theta(n-1)|} + |\hat{\omega}(n)| \underline{x}(n)^{\mathrm{T}} P(n-1) \underline{x}(n)}. \quad (31)$$

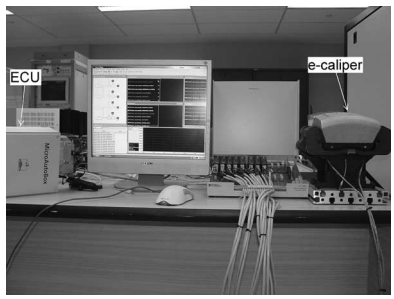

Fig. 5. Our experimental setup, using the brake-by-wire designed at Pacifica Group Technologies Ltd. Pty.

Combining (23), (29)–(31) will result in the following updated formula:

$$\underline{\alpha}(n) = \underline{\alpha}(n-1) + \underline{K}(n) e(n) \quad (32)$$

where

$$e(n) = |\hat{\omega}(n)|^{\frac{1}{2}} \left(y(n) - \underline{\alpha}(n-1)^{\mathrm{T}} \underline{x}(n) \right). \quad (33)$$

Similar to RLS, and in order to accelerate the convergence of the estimates toward the true parameters, the matrix $P(n)$ is initialized to a nonsingular matrix with positive large eigenvalues. For the implementation of the algorithm in this paper, we chose $P(0) = 10^5 I_5$ (I_n is the $n \times n$ identity matrix).

IV. Experimental Results

In order to evaluate the performance of the proposed recursive-estimator design in terms of its accuracy and tracking convergence, we have run a number of experiments using an EMB system that has been recently developed by Pacifica Group Technologies Ltd. Pty. The architecture of the e-caliper and its connections to other components in the EMB system is similar to the diagrams shown in Fig. 2. In addition to recording the resolver output signals through two 12-bit analog-to-digital converters, we added a high-resolution encoder to record the true rotor-position signal and calculate the exact parameters of the characteristic ellipse of the resolver. A photograph of our test-rig is shown in Fig. 5, where two main components of the EMB systems are labeled (the ECU and the e-caliper).

In this paper, we programmed the ECU to send an input command to the position controller that turned the resolver rotor eight full cycles in the positive direction with varying speeds involving several resting periods. We recorded the resolver-data samples at the rate of 250 samples/s. The recorded data samples have been plotted versus each other and shown in Fig. 4, where they orbit an elliptic route (the characteristic ellipse of the resolver).

Fig. 6 shows the true θ signal along with the relative estimation error of A_1 parameter for RLS, RWLS, and MRWLS techniques, where a relative error is defined as the ratio of the absolute error $|\hat{A}_1 - A_1|$ to the true parameter value A_1. There are four resting periods during with which the resolver position θ varies slowly. Each technique needs an initial transient period

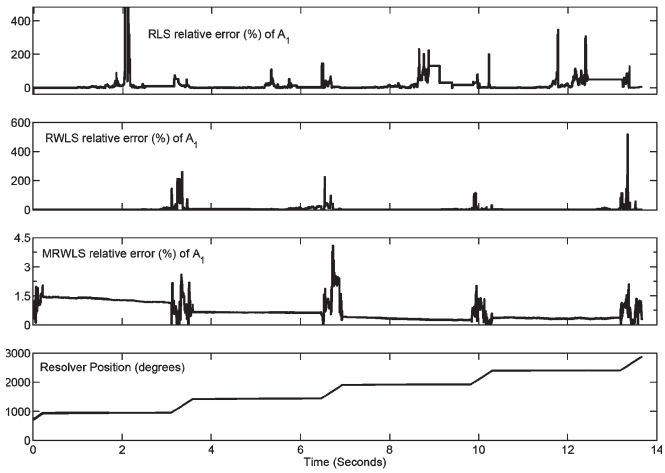

Fig. 6. Resolver true position signal with the relative error of the parameter estimates $\hat{A}_1$ given by RLS, RWLS, and MRWLS techniques.

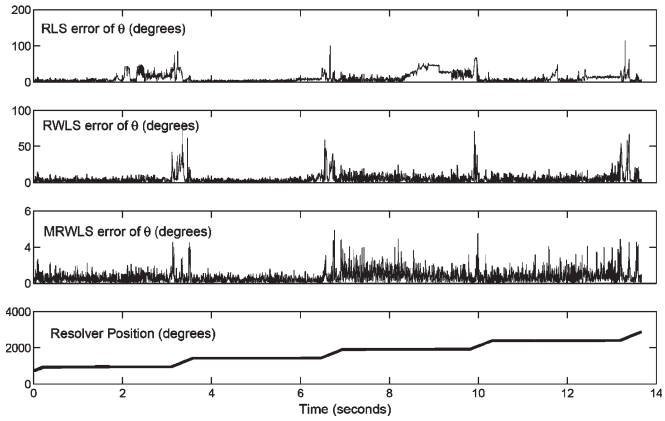

Fig. 7. Resolver true position signal θ with the relative error of the estimated $\hat{\theta}$ values generated by the complete position estimator shown in Fig. 3 with resolver calibration using RLS, RWLS, and MRWLS estimators.

during which the resolver rotor turns almost two cycles and the estimator outputs gradually converge using the recorded data (this period is not shown in Figs. 6 and 7).

We observe that the RLS technique fails during the resting periods and immediately after them with its estimation error increasing up to 400%. Indeed, by using RLS during a long resting period, we mainly include the recent samples, which are concentrated around the resting points, to be fitted to an ellipse. Hence, the resulting ellipse is different from the characteristic ellipse of the resolver and, incorrect resolver-parameter estimates are resulted. After a resting period, as previous data samples are forgotten, the RLS starts to gradually update the parameter estimates using the new scattered data. This is similar to what happens during an initial transient period, and the RLS results in wrong parameter estimates again. The RWLS technique tries to correct the first misbehavior of the RLS estimator during the resting periods by assigning smaller weights to the concentrated data samples recorded during the resting periods, and Fig. 6 confirms that the relative estimation error of the RWLS is not large during these periods. However, the repeated transient periods still exist with the RWLS estimator and increase its error to around 350% after the resting periods.

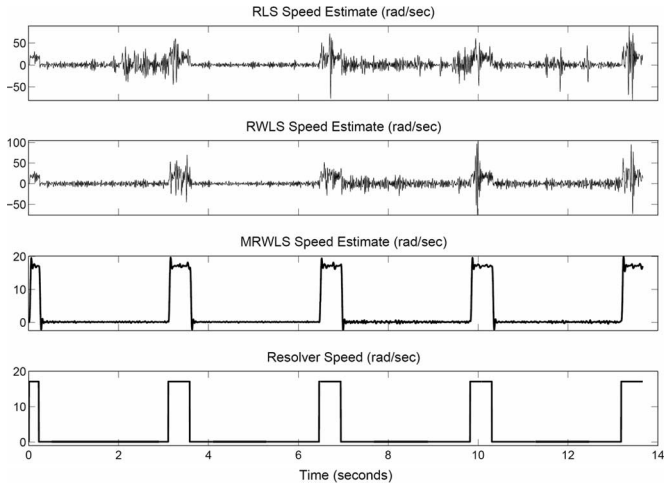

Fig. 8. Resolver true speed signal ω and its estimates $\hat{\omega}$ given by the speed estimator in the scheme shown in Fig. 3 with resolver calibration using RLS, RWLS, and MRWLS estimators.

Using the new MRWLS estimator, we replace the exponent term $n-i$ in (15) with the $g(i,n)$ defined in (19) so that the previous data samples are forgotten only when the resolver rotor is moving. This modification results in a maximum error of 4.5%.

Fig. 7 shows the relative error of the estimated $\hat{\theta}$ values generated by the complete position estimator (shown in Fig. 3) with RLS, RWLS, and MRWLS techniques separately applied to calibrate the resolver. Since the ellipse-parameter estimates, given by the RLS and RWLS, diverge during resting periods and during transient periods after the resting periods, their corresponding actuator-position estimates are substantially erroneous. Indeed, the error of position estimation exceeds 30° during most of the resting periods and occasionally reaches 100°. During such periods, the actuator cannot be controlled and the braking function will fail. On the other hand, the accurate elliptic-parameter estimation performed by MRWLS results in a substantially better estimation of actuator position with the estimation error not exceeding 6° and with root-mean-square value of 1.85°. This error is tolerable in our application, where the main purpose of position control is to maintain a desired clamp force in the e-caliper, based on a given stiffness curve. Fig. 8 shows the true speed of the actuator and the speed estimates $\hat{\omega}$ generated by the speed estimator (shown in Fig. 3) with the RLS, RWLS, and MRWLS techniques separately applied to calibrate the resolver. Due to the divergence of the resolver-parameter estimates given by the RLS and RWLS, their speed estimates substantially deviate from the true speed, while the speed estimate using the resolver parameters given by the MRWLS track the true speed of the actuator.

Our proposed MRWLS technique only requires 41 variables to be saved in the memory and updated in real-time, including the five $\alpha_i(n)$ parameters, five $x_i(n)$, and one $y(n)$ inputs to the algorithm, 25 elements of the matrix $\Phi(n)$, and five elements of the vector $\underline{K}(n)$. Memory requirements of alternative methods, such as Fitzgibbon *et al.* [19], are substantially higher as they are designed for offline ellipse-fitting applications in which the memory and computational power are not scarce. Considering

the low computational complexity of the technique, our experiments on the EMB caliper has shown that for the e-caliper microprocessor, it takes less than 2 ms to update the resolver parameters using the MRWLS technique. This interval is only half of the sampling time, and therefore, the proposed MRWLS can be used in real-time in this application.

V. Conclusion

Resolvers are absolute position transducers applied in a large variety of industrial applications to control the position and speed of actuators. In EMB systems, resolvers are used to sense the position and speed of the actuator in brake calipers. Accuracy and convergence of the position and speed measurements provided by resolvers are essential for reliable braking and the vehicle and driver's safety. Since the parameters of resolvers vary with aging and temperature, an adaptive estimator is required for real-time calibration of these parameters.

When the pair of resolver signals are plotted versus each other, they form an ellipse called the characteristic ellipse of the resolver. This paper investigates the formulation of a straightforward algebraic relationship between the parameters of the characteristic ellipse of the resolver and the resolver parameters. An adaptive estimator is then presented by which parameters of the characteristic ellipse of a resolver are calibrated in real-time using the direct measurements provided by the resolver. The proposed technique is a modified version of a RWLS estimator and has been specially developed to calibrate resolver sensors used in actuator-control applications like EMB systems, for which long resting periods frequently occur. The proposed method can also be applied for real-time calibration of other sensors with elliptic parametrization, such as short-range radars [23].

Experimental results with an EMB e-caliper show that the well-known RLS technique is unable to track the resolver parameters during resting periods (and some transient periods immediately after the resting periods) with its estimation relative error reaching up to 400%. This problem is corrected by adding appropriate weights to the error terms and modifying the forgetting factor in the RLS error function. The proposed method was experimentally evaluated and shown to be capable of providing relatively accurate estimates for the resolver parameters and the actuator position.

References

[1] D. M. Van de Sype, K. De Gusseme, A. P. Van den Bossche, and J. A. Melkebeek, "Duty-ratio feedforward for digitally controlled boost pfc converters," *IEEE Trans. Ind. Electron.*, vol. 52, no. 1, pp. 108–115, Feb. 2005.

[2] L. Deng, F. Janabi-Sharifi, and W. J. Wilson, "Hybrid motion control and planning strategies for visual servoing," *IEEE Trans. Ind. Electron.*, vol. 52, no. 4, pp. 1024–1040, Aug. 2005.

[3] J. W. Ahn, S. J. Park, and D. H. Lee, "Novel encoder for switching angle control of srm," *IEEE Trans. Ind. Electron.*, vol. 53, no. 3, pp. 848–854, Jun. 2006.

[4] Y. Hori, "Future vehicle driven by electricity and control—Research on four-wheel-motored 'uot electric march ii'," *IEEE Trans. Ind. Electron.*, vol. 51, no. 5, pp. 954–962, Oct. 2004.

[5] R. Daily and D. M. Bevly, "The use of GPS for vehicle stability control systems," *IEEE Trans. Ind. Electron.*, vol. 51, no. 2, pp. 270–277, Apr. 2004.

[6] R. Hoseinnezhad and A. Bab-Hadiashar, "Missing data compensation for safety-critical components in a drive-by wire system," *IEEE Trans. Veh. Technol.*, vol. 54, no. 4, pp. 1304–1311, Jul. 2005.

[7] R. Hoseinnezhad, "Position sensing in brake-by-wire calipers using resolvers," *IEEE Trans. Veh. Technol.*, vol. 55, no. 3, pp. 924–932, May 2006.

[8] M. Cirrincione and M. Pucci, "An mras-based sensorless high-performance induction motor drive with a predictive adaptive model," *IEEE Trans. Ind. Electron.*, vol. 52, no. 2, pp. 532–551, Apr. 2005.

[9] C. Lascu, I. Boldea, and F. Blaabjerg, "Comparative study of adaptive and inherently sensorless observers for variable-speed induction-motor drives," *IEEE Trans. Ind. Electron.*, vol. 53, no. 1, pp. 57–65, 2006.

[10] J. Catala i Lopez, L. Romeral, A. Arias, and E. Aldabas, "Novel fuzzy adaptive sensorless induction motor drive," *IEEE Trans. Ind. Electron.*, vol. 53, no. 4, pp. 1170–1178, Jun. 2006.

[11] N. Mutoh, T. Kazama, and K. Takita, "Driving characteristics of an electric vehicle system with independently driven front and rear wheels," *IEEE Trans. Ind. Electron.*, vol. 53, no. 3, pp. 803–813, Jun. 2006.

[12] M. Benammar, L. Ben-Brahim, and M. Alhamadi, "High precision resolver-to-dc converter," *IEEE Trans. Instrum. Meas.*, vol. 54, no. 6, pp. 2289–2296, Dec. 2005.

[13] D. Hanselman, "Resolver signal requirements for high accuracy resolver-to-digital conversion," *IEEE Trans. Ind. Electron.*, vol. 37, no. 6, pp. 556–561, Dec. 1990.

[14] A. Bünte and S. Beineke, "High-performance speed measurement by suppression of systematic resolver and encoder errors," *IEEE Trans. Ind. Electron.*, vol. 51, no. 1, pp. 49–53, Feb. 2004.

[15] B. Höscheler and L. Szael, "Up-to-date technique for easy high-accuracy position acquisition with sinusoidal incremental encoders," *Period. Polytech. Electr. Eng.*, vol. 42, no. 3, pp. 337–345, 1998.

[16] S. Suwankawin and S. Sangwongwanich, "Design strategy of an adaptive full-order observer for speed-sensorless induction-motor drives—Tracking performance and stabilization," *IEEE Trans. Ind. Electron.*, vol. 53, no. 1, pp. 96–119, 2006.

[17] R. J. Wai and K. H. Su, "Adaptive enhanced fuzzy sliding-mode control for electrical servo drive," *IEEE Trans. Ind. Electron.*, vol. 53, no. 2, pp. 569–580, Apr. 2006.

[18] H. J. Shieh, F. J. Lin, P. K. Huang, and L. T. Teng, "Adaptive displacement control with hysteresis modeling for piezoactuated positioning mechanism," *IEEE Trans. Ind. Electron.*, vol. 53, no. 3, pp. 905–914, Jun. 2006.

[19] A. Fitzgibbon, M. Pilu, and R. Fisher, "Direct least square fitting of ellipses," *IEEE Trans. Pattern Anal. Mach. Intell.*, vol. 21, no. 5, pp. 476–480, May 1999.

[20] J. M. Reed and S. Hutchinson, "Image fusion and subpixel parameter estimation for automated optical inspection of electronic components," *IEEE Trans. Ind. Electron.*, vol. 43, no. 3, pp. 346–354, Jun. 1996.

[21] H. Naruse, A. Nobiki, T. Yabuta, and M. Tateda, "High-accuracy multi-viewpoint stereo measurement using the maximum-likelihood method," *IEEE Trans. Ind. Electron.*, vol. 44, no. 4, pp. 571–578, Aug. 1997.

[22] K. S. Hwang and M. Y. Ju, "A propagating interface model strategy for global trajectory planning among moving obstacles," *IEEE Trans. Ind. Electron.*, vol. 49, no. 6, pp. 1313–1322, Dec. 2002.

[23] I. Chuckpaiwong, "Ellipse fitting method in multidimensional space for on-site sensor calibration," in *Proc. IEEE Region 10 Conf.—TENCON*, 2004, vol. A, pp. 685–688.

[24] S. Haykin, "Recursive least-squares algorithm," in *Adaptive Filter Theory*, 4th ed. Englewood Cliffs, NJ: Prentice-Hall, Sep. 2001, ch. 13, pp. 562–588.

[25] K. R. Thompson, P. P. Acarnley, and C. French, "Rotor position estimation in a switched reluctance drive using recursive least squares," *IEEE Trans. Ind. Electron.*, vol. 47, no. 2, pp. 368–379, Apr. 2000.

Reza Hoseinnezhad was born in Tehran, Iran, in 1973. He received the Ph.D. degree from the University of Tehran, Tehran, Iran, in 2002.

Since 2002, he has held various academic positions at both the University of Tehran and Swinburne University of Technology, Hawthorn, Australia. He is currently a Senior Research Fellow with the Faculty of Engineering and Industrial Sciences, Swinburne University of Technology. His research is focused on the development of signal processing and data fusion techniques for drive-by-wire systems and robust estimation techniques for computer vision. He is the holder of two international patents on brake-by-wire systems.

Alireza Bab-Hadiashar (SM'04) was born in Iran in 1964. He received the Ph.D. degree from Monash University, Clayton, Australia, in 1997.

Since 1997, he has held various academic positions at both Monash University and Swinburne University of Technology, Hawthorn, Australia. He is currently an Associate Professor and Program Manager of robotics and mechatronics with the Faculty of Engineering and Industrial Sciences, Swinburne University of Technology. His research interest is in the development of robust data analysis techniques for engineering applications, in general, and computer vision in particular.

Peter Harding was born in Melbourne, Australia, in 1979. He received the B.E. degree in mechatronic engineering from the University of Melbourne, Melbourne, Australia, in 2001.

Since 2001, he has been a Control Engineer with Pacifica Group Technologies, Pty Ltd., East Bentleigh, Australia. His research interests are in electric motor drives and control, and automotive control systems.